DE04F9724

Preprint 2004 - 16
June

Mass measurement on the *rp*-process waiting point ^{72}Kr

D. Rodriguez, V.S. Kolhinen, G. Audi, J Äystö, D. Beck, K. Blaum, G. Bollen, F. Herfurth, A. Jokinen, A. Kellerbauer, H.-J. Kluge, M. Oinonen, H. Schatz, E. Sauvan, S. Schwarz

Gesellschaft für Schwerionenforschung mbH
Planckstraße 1 • D-64291 Darmstadt • Germany
Postfach 11 05 52 • D-64220 Darmstadt • Germany

Mass measurement on the *rp*-process waiting point ^{72}Kr

D. Rodríguez[1*], V.S. Kolhinen[2], G. Audi[3], J. Äystö[2], D. Beck[1], K. Blaum[1,4], G. Bollen[5], F. Herfurth[1], A. Jokinen[2], A. Kellerbauer[4], H.-J. Kluge[1], M. Oinonen[6], H. Schatz[5,7], E. Sauvan[4†], and S. Schwarz[5]
[1] *GSI, Planckstraße 1, 64291 Darmstadt, Germany*
[2] *University of Jyväskylä, P.O. Box 35, 40351 Jyväskylä, Finland*
[3] *CSNSM-IN2P3-CNRS, 91405 Orsay-Campus, France*
[4] *CERN, Physics Department, 1211 Geneva 23, Switzerland*
[5] *NSCL and Dept. of Physics and Astronomy, Michigan State University, East Lansing, MI 48824-1321, USA*
[6] *Helsinki Institute of Physics, P.O. Box 64, 00014 University of Helsinki, Finland and*
[7] *Joint Institute for Nuclear Astrophysics, Michigan State University, East Lansing, MI 48824-1321, USA*
(Dated: June 14, 2004)

The mass of one of the three major waiting points in the astrophysical *rp*-process ^{72}Kr was measured for the first time with the Penning trap mass spectrometer ISOLTRAP. The measurement yielded a relative mass uncertainty of $\delta m/m = 1.2 \cdot 10^{-7}$ ($\delta m = 8$ keV). Other Kr isotopes, also needed for astrophysical calculations, were measured with more than one order of magnitude improved accuracy. We use the ISOLTRAP masses of $^{72-74}$Kr to reanalyze the role of the ^{72}Kr waiting point in the *rp*-process during X-ray bursts.

Masses are among the most critical nuclear parameters in nucleosynthesis calculations in astrophysics [1]. Here we address the rapid proton capture process (*rp*-process) that powers type I X-ray bursts [1–3]. In this scenario, within 10-100 s, hydrogen and helium are fused explosively into heavy elements up to Te. The nuclear energy release typically reaches 10^{39}-10^{40} ergs and generates a bright X-ray burst. The energy generation is dominated by the *rp*-process, a sequence of rapid proton captures interrupted by slow β^+ decays (waiting points) near the proton drip line when further proton captures are counteracted by (γ,p) photodisintegration of weakly proton bound, or proton unbound nuclei. The waiting points delay the nuclear energy release and therefore directly affect the burst shape and duration [4–8]. Brown *et al.* [6] demonstrated that current mass uncertainties for neutron deficient nuclei around the three major waiting points ^{64}Ge, ^{68}Se, and ^{72}Kr lead to large uncertainties in calculations of X-ray burst light curves. Woosley *et al.* [7] came to similar conclusions with a more complex X-ray burst model. Clearly such mass uncertainties are currently the biggest obstacle in the interpretation of the stream of new observational data on X-ray bursts that is now obtained with satellites such as RXTE, Chandra, or XMM-Newton. For example, Galloway *et al.* [9] attempt to extract critical information on the system parameters of the X-ray burster GS 1826-24 from the analysis of long term X-ray burst profile changes that are orders of magnitude smaller than the light curve shape uncertainties from nuclear physics.

In this letter, we address the mass uncertainty affecting the waiting point ^{72}Kr by precision mass measurements of $^{72-74}$Kr with the ISOLTRAP mass spectrometer [10–12], located at the ISOLDE facility [13] at CERN/Geneva (Switzerland). The critical parameter for modeling the X-ray burst light curve is the effective lifetime of ^{72}Kr in the stellar environment. The ^{72}Kr lifetime is the time it takes for an arbitrary initial abundance to drop by $1/e$. It is determined by the rates of β^+ decay and proton capture processes. ^{73}Rb has been shown to be particle unbound [14, 15] and therefore a local (p,γ)-(γ,p) equilibrium between ^{72}Kr and ^{73}Rb is established. The lifetime reduction of ^{72}Kr through proton capture depends then exponentially on the mass difference between ^{72}Kr and ^{73}Rb and linearly on the proton capture rate of ^{73}Rb [1]. However, in the *rp*-process peak temperatures can become sufficiently high for (γ,p) photodisintegration of the proton bound nucleus ^{74}Sr to drive ^{72}Kr, ^{73}Rb, and ^{74}Sr into a local (p,γ)-(γ,p) equilibrium. For the highest temperatures the lifetime reduction of ^{72}Kr through proton capture therefore depends exponentially on the mass difference between ^{72}Kr and ^{74}Sr and linearly on the β^+ decay rate of ^{74}Sr [1]. Thus, accurate masses of ^{72}Kr, ^{73}Rb, and ^{74}Sr are required. We address this need by measuring the $^{72-74}$Kr masses and use fairly accurate theoretical Coulomb shifts to get the masses of ^{73}Rb and ^{74}Sr.

In the experiments described here, the radioactive Kr isotopes (^{72,73,74}Kr) were produced in spallation reactions as a result of bombarding either a ZrO_2 or a Nb foil target, with the intense high-energy proton beam from the CERN PS-Booster accelerator. A short pulse of $3.2 \cdot 10^{13}$ protons with an energy of 1.4 GeV impinged on the target every 2.4 s. A water-cooled transfer line between target and ion source was used such that mainly volatile elements as *e.g.* noble gases were transported into the plasma ion source biased at 60 kV. The High Resolution Separator (HRS) was used with a mass resolving

* *Present address:* IN2P3, LPC-ENSICAEN, 6 Boulevard du Marechal Juin, 14050, Caen Cedex, France.
E-mail: rodriguez@lpccaen.in2p3.fr.
† *Present address:* IN2P3, CPPM, 13288 Marseille, France

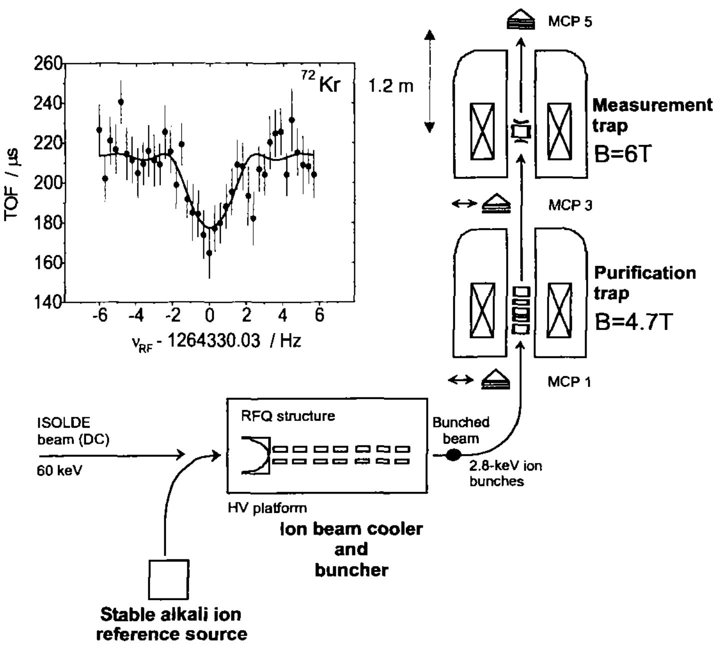

FIG. 1: Sketch of the ISOLTRAP setup. MCP detectors are used to observe the ion beam transfer and to measure the time of flight (MCP5). The inset shows a time-of-flight cyclotron resonance of ^{72}Kr with a fit of the theoretical line-shape [16] to the data points.

power typically of $R \approx 6000$, helping in suppresing isobaric beam contaminations.

The ISOLTRAP system is shown in Fig. 1. It consists of three different traps: a buffer-gas-filled linear Paul trap [11], a gas-filled cylindrical Penning trap [17], and a hyperbolic Penning trap in high vacuum [10].

The 60-keV ISOLDE beam is electrostatically retarded to a few tens of eV and stopped in the buffer-gas-filled linear Paul trap. There, the ions are cooled by collisions with ≈ 0.5 Pa helium buffer gas. After an accumulation time varying from 3 ms (for ^{74}Kr) up to 50 ms (for ^{72}Kr), the cooled ion bunch is ejected with a temporal width of less than 1 μs and an emittance of less than 10π mm mrad at 2.8 keV transfer energy.

The ion bunches are transported and captured in the helium-buffer-gas filled cylindrical purification Penning trap. This trap uses a mass-selective buffer-gas cooling technique for isobaric cleaning of the injected ion bunch [18]. In the ^{72}Kr experiment this trap was operated with a resolving power of 16000. After the isobaric cleaning the ions are ejected and transferred to the precision Penning trap where the actual mass measurement is carried out by the determination of the cyclotron frequency $\nu_c = qB/(2\pi m)$ of stored ions with mass m and charge q in a homogeneous magnetic field B. The ions cyclotron frequency ν_c is probed by exciting the ions' motion by a radiofrequency signal (RF) and measurement of the time of flight to the micro-channel-plate detector MCP5 [19]. Repeating this for different RF frequencies and measuring the time of flight as a function of the RF-frequency, yields a time-of-flight cyclotron resonance curve as shown for $^{72}Kr^+$ in the inset of Fig. 1. The magnetic field calibration B is performed by a determination of the cyclotron frequency of a reference ion ν_c^{ref} with well-known mass both before and after the measurements of the cyclotron frequency of the ion of interest. The value adopted for the cyclotron frequency of the reference ion ν_c^{ref} is the result of the linear interpolation of both measurements (before and after) to the center of the time interval during which the cyclotron frequency of the ion of interest was measured.

The presence of contaminating ions in the measurement trap, produced either in the ISOLDE plasma ion source or created by charge exchange in the ISOLTRAP preparation traps, induces a shift in the cyclotron frequency of the ion of interest. This shift can be corrected for by applying a count rate analysis [20]. The systematic uncertainties to be added to the uncertainties resulting from the measurements, are outcomes from previous measurements carried out with carbon cluster cross reference measurements [21]. This set of measurements led to a relative uncertainty limit of 8×10^{-9}, which is quadratically added to the other uncertainties to get the final value [20].

The atomic mass is determined from the measured ion cyclotron frequencies via the relationship

$$m_{\text{atom}} = r \cdot (m_{\text{atom}}^{\text{ref}} - m_e) + m_e, \qquad (1)$$

where r is the cyclotron frequency ratio between the reference ion and the ion of interest obtained in the experiment. m_e is the electron mass and $(m_{\text{atom}}^{\text{ref}} - m_e)$ is the reference ion mass.

In this experiment the masses of $^{72}Kr^+$, $^{73}Kr^+$, and $^{74}Kr^+$ were measured directly. A test ion source provided the reference isotope $^{85}Rb^+$, which has a relative mass uncertainty of 2×10^{-10} [22]. The measurements on the krypton isotopes were performed by using excitation times T_{RF} of 300 ms or 400 ms. The cyclotron frequency line-width $\Delta\nu_c$(FWHM) is about $1/T_{\text{RF}}$ in a homogeneous magnetic field with $B = 6$ T, thus resulting in resolving powers $m/\Delta m$(FWHM) of about 5×10^5 for singly charged ions. The excitation time for the stable reference ion $^{85}Rb^+$ was $T_{\text{RF}} = 1.2$ s.

The resulting ratios for the cyclotron frequencies are given in Tab. I. The table also gives the mass excess values $D = m_{\text{atomic}} - A \cdot \text{u}$ resulting from the experiments reported here and compares it with those given in the literature [26] published prior to our experiments.

For *rp*-process model calculations the masses of ^{72}Kr, ^{73}Rb, and ^{74}Sr are important. The mass of ^{72}Kr was directly determined in this work (see Tab. I). For the nuclides ^{73}Rb and ^{74}Sr, we obtain a mass excess of $-45.9(0.1)$ MeV and $-40.8(0.1)$ MeV, from our measured masses of the isospin mirrors ^{73}Kr and ^{74}Kr (Tab. I)

TABLE I: Frequency ratios ν_c^{ref}/ν_c relative to $^{85}Rb^+$ and mass excesses (D) for $^{72,73,74}Kr$. The experimental mass excesses (D_{exp}) are determined from the cyclotron frequency ratios using $m(^{85}Rb)$= 84.911 789 738(12) u [22], m_e = 0.000 548 579 9110(12) u [23] and 1 u=931494.009(7) keV [24]. D_{lit} are the AME values from 1995 [26]. The half-lives $T_{1/2}$ are taken from [25].

Nuclide	$T_{1/2}$	ν_c^{ref}/ν_c	D_{exp} (keV)	D_{lit} (keV)	$D_{new} - D_{lit}$ (keV)
^{72}Kr	17.2(3) s	0.847 255 827(101)	−53940.6(8.0)	−54110(270)	159
^{73}Kr	27.0(1.2) s	0.858 999 8172(830)	−56551.7(6.6)	−56890(140)	338
^{74}Kr	11.5(1) min	0.870 703 7406(262)	−62332.0(2.1)	−62170(60)	−162

and using the Coulomb shifts calculated by Brown *et al.* [6]. The uncertainty is entirely determined by the estimated uncertainty for the Coulomb shifts of 100 keV. With these mass values we obtain proton separation energies of −0.7(0.1) MeV for ^{73}Rb and of 2.2(0.1) MeV for ^{74}Sr.

To evaluate the impact of the new mass values on X-ray burst models we calculate the ^{72}Kr lifetime as a function of temperature for a typical density of 10^6 g/cm^3, and a solar hydrogen abundance. For each temperature, we solve the system of differential equations for the abundances of ^{72}Kr, ^{73}Rb, and ^{74}Sr for constant temperature and density as function of time. We take into account proton capture on ^{72}Kr and ^{73}Rb, (γ,p) photodisintegration on ^{73}Rb and ^{74}Sr as well as β^+ decay of ^{72}Kr, ^{73}Rb, and ^{74}Sr.

Proton capture rates were the same as in Schatz *et al.* [5] and were calculated with the statistical Hauser-Feshbach code 'non-smoker' [27]. The inverse photodisintegration rates $\lambda_{(\gamma,p)}$ were calculated from the capture rates $< \sigma v >_{(p,\gamma)}$ and the new reaction Q-values using detailed balance [1]:

$$\lambda_{(\gamma,p)} = \frac{2G_f}{G_i}\left(\frac{\mu kT}{2\pi\hbar^2}\right)^{3/2} e^{-Q/kT} \cdot < \sigma v >_{(p,\gamma)}, \quad (2)$$

where G_i and G_f are the partition functions of the initial and final nuclei for proton capture, μ is the reduced mass for proton capture, k is the Boltzmann constant and T the temperature. We neglect in this analysis the impact of the new masses on the recalculation of the 'non-smoker' proton capture rates. This is justified as the effect is usually small compared to the exponential mass dependence of Eq. (2). Our results for the lifetime of ^{72}Kr are shown in Fig. 2 as upper and lower limits taking into account our new, much improved mass uncertainties. For comparison, Fig. 2 also shows the ^{72}Kr lifetime limits based on the previously known mass data from the AME95 [26]. For low and high temperatures, proton captures are neglegible and the lifetime is entirely given by the β^+ decay. The reason is that for low temperatures, proton captures are too slow while for high temperatures, photodisintegration is too strong. For intermediate temperatures, however, a lifetime reduction due to proton capture can in principle occur, depending on the assumed Q-values.

As Fig. 2 shows, our new mass measurements strongly reduce the Q-value induced uncertainty in the ^{72}Kr *rp*-process lifetime. For the proton capture rates used here we can now exclude the order of magnitude reduction in lifetime around typical X-ray burst peak temperatures of 1-1.5 GK. This is consistent with constraints on the proton separation energy of ^{73}Rb derived from its non-observation in radioactive beam experiments together with assumptions on its production cross section [14]. These constraints can be translated into a lower lifetime limit also displayed in Fig. 2.

In short, our mass measurements show that when using 'non-smoker' proton capture rates the ^{72}Kr lifetime in the *rp*-process will always be within 80% of its β^+ half-life. In most models, the reduction will be less, as densities during the burst tend to drop somewhat below 10^6 g/cm^3 due to expansion, and the hydrogen abundance tends to be reduced compared to the solar value

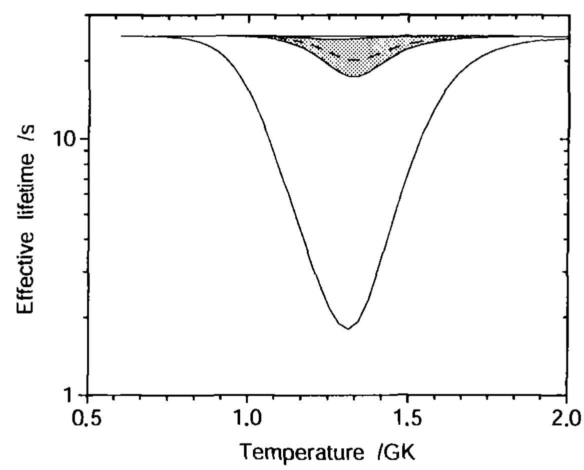

FIG. 2: The effective lifetime of ^{72}Kr in the stellar environment as a function of temperature for typical *rp*-process conditions. The solid lines delimit the range of lifetimes within the old AME95 mass uncertainties. The grey area marks the range of lifetimes within the new mass uncertainties obtained in this work. The dashed line is the lower limit from the non-observation of ^{73}Rb.

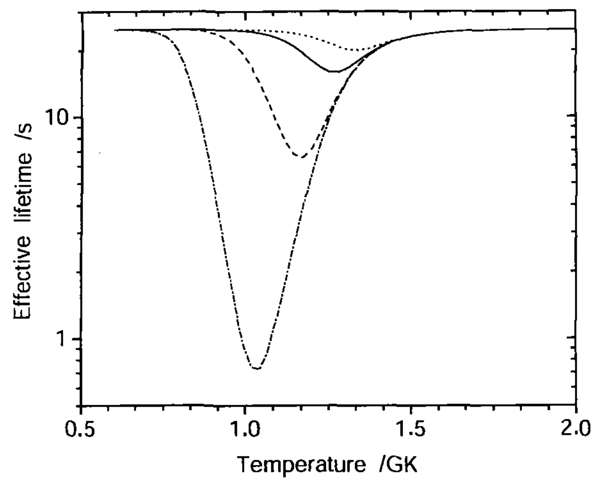

FIG. 3: The lower limit of the effective lifetime of ^{72}Kr as a function of temperature for typical *rp*-process conditions calculated with the masses of this work and taking into account the experimental non-observation of ^{73}Rb. Here, the ^{73}Rb(p,γ)^{74}Sr reaction rate has been multiplied by factors of 1 (dotted), 5 (solid), 100 (dashed), and 10000 (dot dashed).

at the time the reaction flow reaches ^{72}Kr. The nuclide ^{72}Kr remains therefore a strong waiting point in the *rp*-process during X-ray bursts delaying energy generation with at least 80% of its β^+ decay half-life. This strengthens further the hypothesis that long burst durations imply hydrogen rich bursts with an *rp*-process reaching the $A = 64 - 72$ mass region. However, our new mass measurements suggest a fairly high proton separation energy for ^{74}Sr of 2.18 MeV (previously 1.69 MeV). Therefore (γ,p)-photodisintegration of ^{74}Sr sets in at rather high temperatures around 1.3-1.4 GK. This results in a fairly wide temperature window where it is hot enough for proton captures to matter, but where only ^{72}Kr and ^{73}Rb, and not ^{74}Sr participate in the local (p,γ)-(γ,p) equilibrium. In that regime, the ^{72}Kr lifetime depends also on the ^{73}Rb(p,γ) reaction rate. In fact, as Fig. 3 shows, an increase of the ^{73}Rb(p,γ) reaction rate by factors of 100 or more could entirely compensate the reduction in proton capture flow due to a more unbound ^{73}Rb. Uncertainties of many orders of magnitude cannot be entirely excluded for proton capture rates near the proton dripline, where usually a few resonances dominate (see *e.g.* [28]). As a consequence of our new mass measurements we therefore have to conclude, that for reliable *rp*-process calculations the ^{73}Rb(p,γ)^{74}Sr reaction rate needs to be known to better than a factor of 2-3. This requires experimental information. As ^{73}Rb is a fast proton emitter with a lifetime of less than 24 ns the reaction rate cannot be determined directly. It would be important to measure in future experiments the masses of ^{73}Rb and ^{74}Sr, as well as the level structure of ^{74}Sr in the vicinity of the proton threshold with keV precision. For ^{73}Rb the mass could be measured using a (p,d) transfer reaction in inverse kinematics with a radioactive ^{74}Rb beam or β-delayed proton decay of ^{73}Sr.

H.S. is an Alfred P. Sloan fellow, and acknowledges support through NSF grants PHY 02-16783 (Joint Institute for Nuclear Astrophysics) and PHY 01-10253. G.B. and S.S. acknowledge support through NSF grant PHY 01-10253. We thank B.A. Brown for providing the calculated Coulomb shifts, and F.-K. Thielemann for providing the reaction network solver. This work was supported by the European Commission within the EUROTRAPS network under contract number ERBFM RXCT97-0144, the RTD project EXOTRAPS under contract number HPRI-CT-1998-00018, and the NIPNET network under contract number HPRI-CT-2001-50034.

[1] H. Schatz *et al.*, Phys. Rep. 294 (1998) 167.
[2] R.K. Wallace and S.E. Woosley, Astrophys. J. (Suppl.) 45 (1981) 389.
[3] T. E. Strohmayer and L. Bildsten, in Compact Stellar X-ray Sources, eds. W.H.G. Lewin and M. van der Klis, Cambridge University Press, astro-ph/0301544, 2003.
[4] O. Koike, M. Hashimoto, K. Arai, and S. Wanajo, Astron. Astrophys. 342 (1999) 464.
[5] H. Schatz *et al.*, Phys. Rev. Lett. 86 (2001) 3471.
[6] B. A. Brown *et al.* Phys. Rev. C 65 (2002) 5802.
[7] S. E. Woosley *et al.*, astro-ph/0307425 (2003).
[8] J. L. Fisker and F.-K. Thielemann, astro-ph/0312361 (2003).
[9] D. K. Galloway *et al.*. astro-ph/0308122 (2003).
[10] G. Bollen *et al.*, Nucl. Instrum. Methods A 368 (1996) 675.
[11] F. Herfurth *et al.*, Nucl. Instrum. Methods A 469 (2001) 254.
[12] K. Blaum *et al.*, Nucl. Instrum. Methods B 204 (2003) 478.
[13] E. Kugler, Hyp. Int. 129 (2000) 23.
[14] R. Pfaff *et al.*, Phys. Rev. C 53 (1996) 1753.
[15] A. Jokinen *et al.*, Z. Phys. A 355 (1996) 227.
[16] M. König *et al.* Int. J. Mass Spectrom. Ion Processes 142 (1995) 95.
[17] H. Raimbault-Hartmann *et al.*, Nucl. Instrum. Methods B 126 (1997) 378.
[18] G. Savard *et al.*, Phys. Lett. A 158 (1991) 247.
[19] G. Gräff, H. Kalinowsky, and J. Traut, Z. Phys. A 297 (1980) 35.
[20] A. Kellerbauer *et al.*, Eur. Phys. J. D 22 (2003) 53.
[21] K. Blaum *et al.*, Eur. Phys. J. A 15 (2002) 245.
[22] M.P. Bradley *et al.*, Phys. Rev. Lett. 83 (1999) 4510.
[23] P.J. Mohr and B.N. Taylor, J. Phys. Chem. Ref. Data 28 (1999) 1713.
[24] G. Audi, Hyp. Int. 132 (2001) 7.
[25] G. Audi, O. Bersilon, J. Blachot, and A.H. Wapstra, Nucl. Phys. A 624 (1997) 1.
[26] G. Audi and A.H. Wapstra, Nucl. Phys. A 595 (1995) 409.
[27] T. Rauscher and F.-K. Thielemann, At. Data Nucl. Data Tables 75 (2000) 1. The rates were recalculated by T. Rauscher using the masses given in the 1995 Atomic Mass Evaluation [26].
[28] R.R.C. Clement *et al.*, Phys. Rev. Lett. 92 (2004) 172502.